NJC

Accepted Manuscript

This is an *Accepted Manuscript*, which has been through the Royal Society of Chemistry peer review process and has been accepted for publication.

Accepted Manuscripts are published online shortly after acceptance, before technical editing, formatting and proof reading. Using this free service, authors can make their results available to the community, in citable form, before we publish the edited article. We will replace this *Accepted Manuscript* with the edited and formatted *Advance Article* as soon as it is available.

You can find more information about *Accepted Manuscripts* in the Information for Authors.

Please note that technical editing may introduce minor changes to the text and/or graphics, which may alter content. The journal's standard Terms & Conditions and the Ethical guidelines still apply. In no event shall the Royal Society of Chemistry be held responsible for any errors or omissions in this *Accepted Manuscript* or any consequences arising from the use of any information it contains.

ROYAL SOCIETY OF CHEMISTRY

www.rsc.org/njc

Journal Name

ARTICLE

Vacuum-depositable thiophene- and benzothiadiazole-based donor materials for organic solar cells

Received 00th January 20xx,
Accepted 00th January 20xx

DOI: 10.1039/x0xx00000x

www.rsc.org/

Yongjun Jeon,[†a] Tae-Min Kim,[†b] Jang-Joo Kim[*b] and Jong-In Hong[*a]

Three (D–A–D)-type electron donor materials, containing 2,1,3-benzothiadiazole as the electron-withdrawing core, and benzothiophene, naphthalene, and thiophene as electron-donating terminal groups, were synthesized for vacuum-depositable small-molecule organic solar cells. The donor material containing thiophene as the terminal group, **DT**, shows a maximum power conversion efficiency of 4.13%, a short-circuit current density of 9.89 mA cm^{-2}, an open-circuit voltage of 0.86 V, and a fill factor of 0.48, on bulk heterojunction solar cell with a blend ratio of **DT**:C_{70} = 1:4 under simulated AM 1.5 solar irradiation at 100 mW cm^{-2}.

Introduction

Organic photovoltaics (OPVs) convert solar energy to electrical energy and thus have attracted considerable interest as a possible alternative to conventional inorganic photovoltaics. OPV devices have several advantages over inorganic solar cells, such as mechanical flexibility, easy synthesis of active-layer materials, light weight, and low manufacturing cost. Owing to these advantages, intensive research towards the development of OPV devices has been conducted,[1] in spite of their lower power conversion efficiencies (PCE) compared to inorganic solar cells.

The PCE of p-n junction OPVs can be increased by facilitating exciton diffusion and exciton dissociation, using bulk heterojunction (BHJ) structure and fullerene derivatives, respectively.[2] Current studies on OPVs are usually focused on enhancing their PCEs using novel electron donor materials. A general method for enhancing the PCE of OPVs using organic electron donors is by improving the light harvesting ability, which can be generally achieved by broadening the absorption ranges or by increasing the molar extinction coefficients. Usually, broadening absorption ranges is easier and more efficient than increasing molar extinction coefficients.

In this study, we have designed and synthesized three donor–acceptor–donor (D–A–D)-type organic electron donor molecules (**NP**, **BT**, and **DT**) to broaden the light absorption ranges, consisting of 2,1,3-benzothiadiazole as the electron-withdrawing core,[3,4] and benzothiophene, naphthalene, and thiophene as the electron-donating terminal groups. Two thiophene units were used as spacers between the electron-withdrawing core and the electron-donating terminal groups, because of the good hole/electron transporting ability of oligothiophenes.[5-7] It is well known that intramolecular charge transfer (ICT) in a D–A-type molecule lowers the HOMO/LUMO energy level gap and thus induces broad strong absorption with a bathochromic shift in addition to its own π–π* absorption band.[8] The three donor molecules have relatively broad absorption ranges due to ICT and have good intermolecular interaction due to their relatively flat structures. BHJ OPV devices fabricated using a blend ratio of **DT**:C_{70} = 1:4 exhibited a maximum PCE of 4.13%.

Experimental

Instruments

^{1}H NMR spectra were recorded in $CDCl_3$ or DMSO using an Avance 300 MHz or 500 MHz Bruker spectrometer. Mass spectra were obtained using a Bruker MALDI-TOF mass spectrometer. Elemental analysis was performed with a Carlo-Erba model EA 1112 elemental analyser. Thermogravimetric analysis (TGA) was performed with a TA instrument model Q-5000 IR. UV-Vis spectra were recorded on a Beckman DU 650 spectrophotometer. Fluorescence spectra were recorded on a Jasco FP-7500 spectrophotometer. For solid-state measurements, the materials were thermally vapour-deposited onto quartz plates in a vacuum chamber to form 40-nm-thick films. The cyclic voltammetric (CV) apparatus used was a CH Instruments model 650B electrochemical workstation. Cyclic voltammograms were obtained at room temperature in a three-electrode cell with a glassy carbon working electrode, a Ag/Ag^+ (0.01 M) reference electrode, and a Pt counter electrode, in dichloromethane or dimethylformamide containing tetrabutylammonium

[a] Department of Chemistry, Seoul National University, Seoul 151-747, Korea; Fax: 82-2-889-1568; Tel: +82-2-880-6682; E-mail: jihong@snu.ac.kr.
[b] WCU Hybrid Materials Program, Department of Materials Science and Engineering and the Centre for Organic Light Emitting Diode, Seoul National University, Seoul 151-742, Korea; E-mail: jjkim@snu.ac.kr.
† These authors contributed equally.

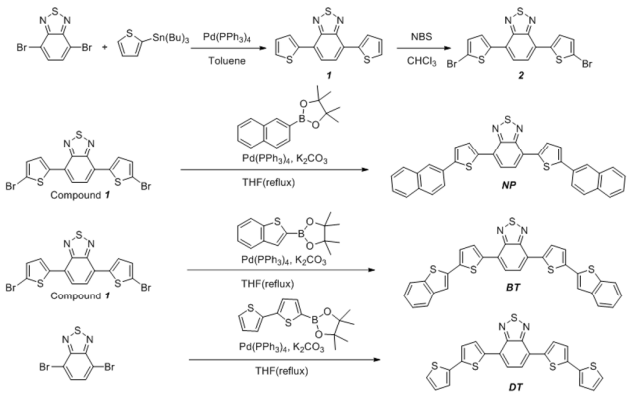

Scheme 1. Synthesis of **BT**, **DT**, **NP**

hexafluorophosphate (0.1 M) as a supporting electrolyte, at a scan rate of 100 mV s^{-1}. All potentials were calibrated with the standard ferrocene/ferrocenium (Fc/Fc^{+}) redox couple. X-ray diffraction spectra were obtained by D8 ADVANCE with DAVINCI, BRUKER. Molecular structures at ground state and the HOMO/LUMO energy levels were calculated using Gaussian 09 Rev. B01 with the DFT/B3LYP method with the 6-31G basis set.

Reagents and materials

All chemicals, such as 4,7-dibromo-2,1,3-benzothiadiazole, 2-(tributylstannyl)thiophene, *N*-bromosuccinimide (NBS), were purchased from either Sigma-Aldrich or Tokyo Chemical Industry (TCI) and were used as received. 4,7-Bis(bromothiophen-2-yl)-2,1,3-benzothiadiazole (***1***) was synthesized according to literature procedure.[9]

Synthesis

Compound 2. To a solution of compound ***1*** (410 mg, 1.36 mmol) in chloroform (30 mL), NBS (730 mg, 4.08 mmol) was added and the mixture was stirred for 12 h at room temperature. Precipitates formed were filtered by a Büchner funnel to give 570 mg of compound ***2*** (yield: 91%).[10]

BT. A mixture of compound ***1*** (1.6 g, 3.5 mmol), 2-(benzo[b] thiophen-2-yl)-4,4,5,5-tetramethyl-1,3,2-dioxaborolane (1.6 g, 8.7 mmol), tetrakis(triphenylphosphine)palladium(0) (40 mg, 0.03 mmol) and potassium carbonate (3.4 g, 24 mmol) in THF/H_2O (100 mL/50 mL) was heated at 70 °C for 72 h. Then the reaction mixture was cooled to room temperature and vacuum filtered using a Büchner funnel to obtain the crude product (yield: 1.20 g, 61%) that was purified by sublimation. ^{1}H NMR (500 MHz, DMSO-d_6): δ (ppm) 7.40 (q, J = 8 Hz, 4H), 7.59 (s, 2H), 7.76 (s, 2H), 7.88 (d, J = 7.5 Hz, 2H), 7.91 (d, J = 8 Hz, 2H), 7.95 (d, J = 7.5 Hz, 2H), 8.17 (s, 2H). T_d: 401.92 °C. HRMS (FAB) *m/z*: calc. for $C_{30}H_{16}N_2S_5$ $[M]^+$: 563.9917, found: 563.9908. Elemental Analysis calc.: C, 63.80; H, 2.86; N, 4.96; S, 28.39; found: C, 63.78; H, 2.84; N, 4.85; S, 28.46.

NP. A mixture of compound ***1*** (1 g, 2.2 mmol), 4,4,5,5-tetramethyl-2-(naphthalen-2-yl)-1,3,2-dioxaborolane (1 g, 5.5 mmol), tetrakis(triphenylphosphine)palladium(0) (25 mg, 0.02 mmol) and potassium carbonate (2.1 g, 15 mmol) in THF/H_2O (100 mL/50 mL) was heated at 70 °C for 72 h. Then, the reaction mixture was cooled to room temperature and vacuum filtered using a Büchner funnel to obtain the crude product (yield: 1.00 g, 83%) that was purified by sublimation. ^{1}H-NMR (500 MHz, DMSO-d_6): δ (ppm) 7.55 (t, J = 18 Hz, 2H), 7.78 (s, 1H), 7.93 (d, J = 7 Hz, 2H) 8.00 (d, J = 4.5 Hz, 2H), 8.18 (s, 1H), 8.23(s, 1H), 8.29 (s, 1H). T_d: 432.87 °C. HRMS (FAB) *m/z*: calc. for $C_{34}H_{20}N_2S_3$ $[M]^+$: 552.0789, found: 552.0789. Elemental Analysis calc.: C, 73.88; H, 3.65; N, 5.07; S, 17.40; found: C, 73.86; H, 3.59; N, 5.00; S, 17.49.

DT. A mixture of 4,7-dibromo-2,1,3-benzothiadiazole (100 mg, 0.34 mmol), 2,2'-bithiophene-5-boronic acid pinacol ester (250 mg, 0.85 mmol), tetrakis(triphenylphosphine)palladium(0) (20 mg, 0.02 mmol) and potassium carbonate (470 mg, 3.4 mmol) in THF/H_2O (50 mL/25 mL) was heated at 70 °C for 72 h. Then, the reaction mixture was cooled to room temperature and vacuum filtered using a Büchner funnel to obtain the crude product (yield: 43 mg, 28%) that was purified by sublimation.

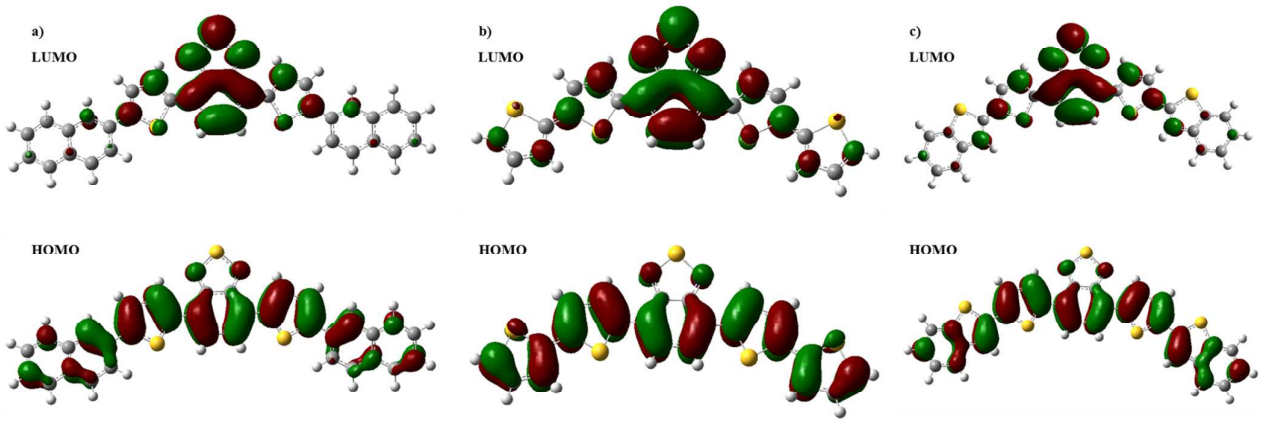

Fig. 1 Molecular orbital surfaces of the HOMO and LUMO of a) ***NP***, b) ***DT*** and c) ***BT***, obtained by the DFT/B3LYP method with the 6-311G(d,p) basis set.

Table 1. Optical, electrochemical and calculation data of **BT**, **DT** and **NP**

Donors	λ_{abs} (nm)[a]	λ_{abs} (nm)[b]	FWHM (nm)[a]	FWHM (nm)[b]	ΔE_{opt} (eV)[a]	HOMO[c] (eV)	LUMO[c] (eV)	ΔE^c (eV)	HOMO[d] (eV)	LUMO[d] (eV)	ΔE^d (eV)
BT	362, 502	342, 475	106	170	2.2	−5.19	−3.17	2.20	-	-	-
DT	356, 502	367, 527	101	148	2.2	−5.13	−3.10	2.03	−5.28	−3.43	1.85
NP	356, 499	363, 518	104	142	2.23	−5.12	−3.01	2.11	−5.40	−3.50	1.90

[a]In Solution; [b]in thin film; [c]calculation data; [d]experimental data from cyclic voltammetry.

^{1}H NMR (300 MHz, $CDCl_3$): δ (ppm) 8.07 (d, J = 3.89 Hz, 2H), 7.89 (2H), 7.33 (d, J = 3.5 Hz, 2H), 7.30 (d, J = 3.72, 4H), 7.09 (t, J = 4.34, 2H). T_d: 367.38 °C. HRMS (FAB) *m/z*: calc. for $C_{22}H_{12}N_2S_5$ $[M]^+$: 463.9604 found: 463.9603. Elemental Analysis calc.: C, 56.87; H, 2.60; N, 6.03; S, 34.50; found: C, 56.77; H, 2.53; N, 6.05; S, 34.66.

Device fabrication

We fabricated planar heterojunction (PHJ) and bulk heterojunction (BHJ) devices (4 mm^2) with configurations of ITO (150 nm) / MoO_3 (5 nm) / Donor (10 nm) / C_{70} (40 nm) / 2,9-dimethyl-4,7-diphenyl-1,10-phenathroline (BCP) (8 nm) / Al (100 nm) and ITO (150 nm) / MoO_3 (5 nm) / Donor:C_{70} (1:1, 1:4; 50 nm) / C_{70} (40 nm) / BCP (8 nm) / Al (100 nm), respectively. On these devices, MoO_3 was used as the hole-injection layer, fullerene derivative was used as the acceptor, and BCP was used as the exciton blocking layer. All layers were prepared by vacuum deposition.

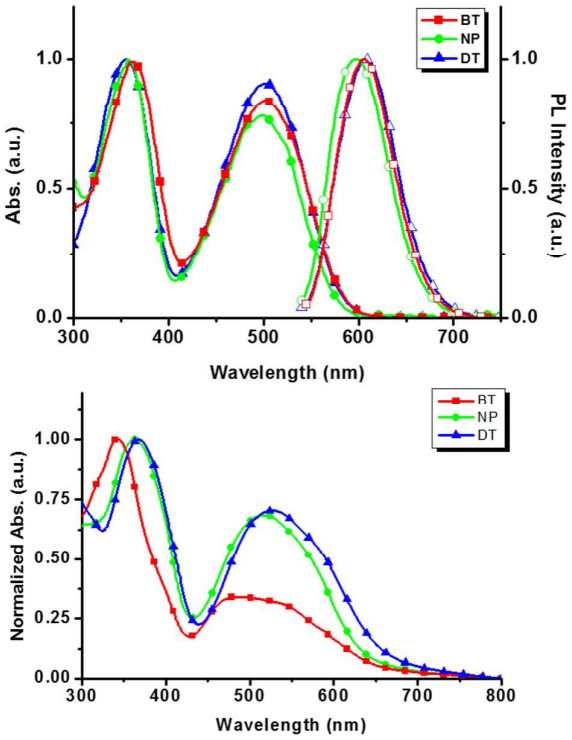

Fig. 2 Absorption spectra and PL spectra of donor materials in a) CH_2Cl_2 and b) thin film. Filled shape indicates absorption spectra and empty shape indicates photoluminescence spectra. (square: **BT**, circle: **NP**, triangle: **DT**)

Calculations

To investigate the correlation between the molecular structure and the photophysical properties, we performed molecular orbital calculations using density functional theory (DFT). The ground state geometries and the molecular orbital distributions of these molecules were optimized in vacuum using the DFT/B3LYP method with the 6-311G(d,p) basis set in the Gaussian 09' B.01 package. **Fig. 1** shows electron density distributions of the HOMOs and LUMOs of the three donor molecules. All of them have broad electron density distributions at the HOMO levels, and localized electron distribution in the benzothiadiazole core region at the LUMO levels. Calculations predicted that these donor molecules will show absorption bands resulting from ICT. The HOMO and LUMO energy levels of donor molecules are stated on Table 1; the LUMO energy levels are high enough to transfer electrons to the acceptor molecule, C_{70}.[11]

Results and discussion

Photophysical and Physical properties

New D-A-D type electron donor materials (***BT***, ***NP*** and ***DT***) were synthesized by the palladium catalysed Suzuki coupling reaction between compound **1** (for **NP** and **BT**) or 4,7-dibromo-2,1,3-benzothiadiazole (for **DT**) and aryl boronate according to **Scheme 1**. **Fig. 2** shows the ultraviolet-visible absorption (UV-vis) and photoluminescence (PL) spectra of three donor materials in solution and as solid films. The three donor materials show the first absorption maxima at 356 nm (**DT**, **NP**) and at 362 nm (**BT**) due to π–π^* transition of terminal groups and the second absorption maxima at 502 nm (**DT**, **BT**) and 499 nm (**NP**) due to ICT. Between the solution-state and solid-film-state spectra of the three donor molecules, there are no significant changes in the first and second absorption bands, but band broadening is observed, which can be measured by the full-width at half-maximum (FWHM). **NP** shows a maximum at 518 nm with a FWHM of 142 nm (104 nm in solution), **DT** shows a maximum at 527 nm with a FWHM of 148 nm (101 nm in solution) and **BT** shows a maximum at 475 nm with a FWHM of 170 nm (106 nm in solution). Three donor materials show a high thermal stability of T_d over 350 °C, as revealed by the TGA thermograms (**Fig. S7-9**), although **DT** is least stable among three materials presumably due to the absence of alkyl termination moieties in the thiophene end-groups. The cyclic voltammograms of three donor materials show irreversible redox process in dichloromethane or dimethylformamide (**Fig. S10**).

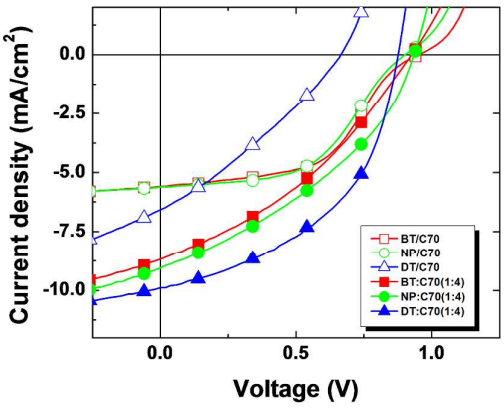

Fig. 3 J-V characteristic plots for OPV devices. Empty shape indicates PHJ devices [ITO (150 nm) / MoO_3 (5 nm) / Donor (10 nm) / C_{70} (35 nm) / BCP (8 nm) / Al (100 nm)]. Filled shape indicates BHJ devices [ITO (150 nm) / MoO_3 (5 nm) / Donor:C_{70} (1:4; 50 nm) / BCP (8 nm) / Al (100 nm)]. (square: **BT**, circle: **NP**, triangle: **DT**)

Photovoltaic cell properties

We fabricated the PHJ and BHJ devices as described in the experimental section. For the PHJ devices, donor layer thickness varies from 10 to 30 nm. **Fig. 3** shows the current density vs. voltage (J–V) characteristics of the PHJ and BHJ devices fabricated using each donor material. **NP**- and **BT**-based PHJ devices show higher performance with a 10-nm-thick donor layer rather than with a thicker donor layer (**Fig S1-3** and **Table S1-3**). This is presumably because their HOMO energy level is too low relative to the transparent conducting oxide (TCO). This is also reflected in the S-shaped curves at the intercept on the voltage axis of the J–V plots as shown in **Fig. S2-3**. Electrochemical experiment data also support that **NP** has deep-lying HOMO relative to TCO (valence energy level −4.8 eV) (**Table 1**).[11] Atomic force microscopy (AFM) images of **DT**, **NP**, and **BT** films clearly indicate the greater tendency of **DT** to form larger aggregates (**Fig. S4**) compared to **NP** and **BT**, which presumably results in less efficient exciton dissociation at the interface for **DT**-based PHJ devices and thus lowers the fill factor (0.30) and decreases PCE (1.32%) in spite of higher current density (J_{sc}) (6.58 mA/cm^2) (**Table 2**).

Table 2. Characteristic solar cell data of heterojunction OPV devices.

Donors	J_{sc} (mA/cm^2)	V_{oc} (V)	FF	PCE (%)
NP 10 nm	5.62	0.92	0.50	2.56
NP:C_{70} 1:4[a]	8.99	0.93	0.37	3.11
DT 10 nm	6.58	0.67	0.30	1.32
DT:C_{70} 1:4[a]	9.89	0.86	0.48	4.13
BT 10 nm	5.61	0.94	0.51	2.69
BT:C_{70} 1:4[a]	8.60	0.94	0.35	2.81

[a] The thickness of active layers of all BHJ devices is 50 nm.

In general, PHJ devices show lower J_{sc} values compared to BHJ devices, because they have narrower exciton dissociation area than BHJ ones.[12] Therefore, we fabricated devices co-deposited with C_{70} to improve J_{sc} by increasing the interfacial area between the electron donor and the electron acceptor. As expected, co-deposited devices show higher J_{sc} values for all devices at a blend ratio **BT** or **NP** or **DT**:C_{70} = 1:4, compared to those of the PHJ devices. This tendency is also observed in the incident photon-to-current efficiency (IPCE) plots (**Fig. S5**). The degree of PCE enhancement of **NP**- and **BT**-based BHJ devices compared to the PHJ devices is always less than the increase in current density, because BHJ devices exhibit lower fill factor values. The lower fill factor values of **NP**- and **BT**-based BHJ devices result from the increased series resistances of BHJ devices compared to those of PHJ devices (**Table S2-3**). For example, the series resistance of **BT**-based BHJ device (**BT**:C_{70} = 1:4, 50 nm, 13.36 Ω/cm^2) is larger than that of **BT**-based PHJ device (**BT** 10 nm/C_{70} 35 nm, 2.30 Ω/cm^2) (Table S2). This tendency is also observed in the case of **NP**-based devices (**Table S3**). The larger series resistances of **BT**- and **NP**-based BHJ devices are due to the mixed layer. Co-deposited layers generate more interfaces compared to the PHJ layers, which increases not only the photo-current density,[13] but also the electrical resistance owing to discrete domains, increased contact resistance, and longer electrical pathway.[14] The fact that **DT**-based BHJ devices display better PCE values than **NP**-based BHJ devices can be rationalized by the AFM images of **DT**:C_{70}- and **NP**:C_{70}-blended films, which clearly show different domain sizes (**Fig. 4**). The **DT**:C_{70}-blended film with a larger domain compared to the **NP**:C_{70}-blended film generates smaller interfacial area, which results in lower electrical

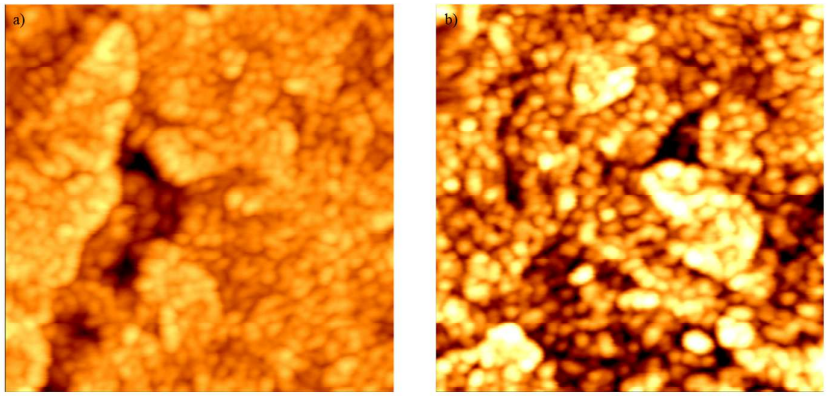

Fig. 4 AFM images of a) **DT**:C_{70}, b) **NP**:C_{70} deposited thin films. The film thickness is 50 nm, mixing ratio is 1:4 = **donor**:C_{70}, and scope range is 1000 nm×1000 nm.

resistance. Another reason for the lower electrical resistance of the **DT**-based BHJ devices was revealed by X-ray diffraction (XRD) spectroscopy. The XRD spectrum of **DT**:C_{70}-blended film shows a well-preserved C_{70} aggregation peak ($2\theta = 21°$)[15-16] compared to the **NP**:C_{70}-blended film (**Fig. S6**). This implies that C_{70} preserves good crystalline morphology even in the **DT**:C_{70}-blended film, thereby facilitating electron extraction.[17]

Conclusions

Three D–A–D-type electron donor materials (**NP**, **DT**, and **BT**), consisting of 2,1,3-benzothiadiazole as the electron withdrawing core, and benzothiophene, naphthalene, and thiophene as the electron donating terminal groups, were designed and synthesised for vacuum-depositable small-molecule organic solar cells. The maximum open-circuit voltage, short-circuit current density, and power conversion efficiency values of the bulk heterojunction device based on **DT**:C_{70} = 1:4 were 0.86 V, 9.89 mA cm^{-2}, and 4.13%, respectively, under simulated AM 1.5 solar irradiation at 100 mW cm^{-2}.

Acknowledgements

This work was supported by the NRF grant (No. 2013R1A1A2074468) funded by the MSIP.

Notes and references

1 (a) Y.-H. Chen, C.-W. Chen, Z.-Y. Huang, K.-T. Wong, L.-Y. Lin, F. Lin and H.-W. Lin, *Org. Electron.*, 2014, **15**, 1828-1835; (b) Y.-H. Chen, L.-Y. Lin, C.-W. Lu, F. Lin, Z.-Y. Huang, H.-W. Lin, P.-H. Wang, Y.-H. Liu, K.-T. Wong, J. Wen, D. J. Miller and S. B. Darling, *J. Am. Chem. Soc.*, 2012, **134**, 13616-13623; (c) S.-W. Chiu, L.-Y. Lin, H.-W. Lin, Y.-H. Chen, Z.-Y. Huang, Y.-T. Lin, F. Lin, Y.-H. Liu and K.-T. Wong, *Chem. Commun.*, 2012, **48**, 1857-1859; (d) L.-Y. Lin, Y.-H. Chen, Z.-Y. Huang, H.-W. Lin, S.-H. Chou, F. Lin, C.-W. Chen, Y.-H. Liu and K.-T. Wong, *J. Am. Chem. Soc.*, 2011, **133**, 15822-15825; (e) L.-Y. Lin, C.-W. Lu, W.-C. Huang, Y.-H. Chen, H.-W. Lin and K.-T. Wong, *Org. Lett.*, 2011, **13**, 4962-4965.

2 (a) H. Hoppe and N. Sariciftci, *J. Mater. Res.*, 2004, **19**, 1924-1945; (b) G. Yu, J. Gao, J.C. Hummelen, F. Wudl and A.J. Heeger, *Science*, 1995, **270**, 1789-1791; (c) N. S. Sariciftci, L. Smilowitz, A. J. Heeger and F. Wudl, *Science*, 1992, **258**, 1474-1476.

3 A. Zitzler-Kunkel, M. Lenze, N. Kronenberg, A.-M. Krause, M. Stolte, K. Meerholz and F. Würthner, *Chem. Mater.*, 2014, **26**, 4856-4866.

4 Y. Chen, Z. Du, W. Chen, S. Wen, L. Sun, Q. Liu, M. Sun and R. Yang, *New J. Chem.*, 2014, **38**, 1559-1564.

5 R. Fitzner, E. Reinold, A. Mishra, E. Mena-Osteritz, H. Ziehlke, C. Körner, K. Leo, M. Riede, M. Weil, O. Tsaryova, A. Weiß, C. Uhrich, M. Pfeiffer and P. Bäuerle, *Adv. Funct. Mater.*, 2011, **21**, 897–910.

6 R. Fitzner, E. Mena-Osteritz, K. Walzer, M. Pfeiffer and P. Bäuerle, *Adv. Funct. Mater.*, 2015, **25**, 1845-1856.

7 H.-Y. Kong, D.-S. Chung, I.-N. Kang, E.-H. Lim, Y.-K. Jung, J.-H. Park, C.-E. Park and H.-K. Shim, *Bull. Kor. Chem. Soc.*, 2007, **28**, 1945–1950.

8 S. Roquet, A. Cravino, P. Leriche, O. Alévêque, P. Frère and J. Roncali, *J. Am. Chem. Soc.*, 2006, **128**, 3459-3466.

9 Y. Yamashita, K. Suzuki and M. Tomura, *Synth. Met.*, 2003, **133-134**, 341–343.

10 X. Zhao, C. Piliego, B. Kim, D. Poulsen, B. Ma, D. Unruh and J. Fréchet, *Chem. Mater.*, 2010, **22**, 2325-2332.

11 W. Zhou, S. Xie, S. Qian, T. Zhou, R. Zhao, G. Wang, L. Qian and W. Li, *J. App. Phys.*, 1996, **80**, 459–463.

12 V. Singh, C. K. Suman and S. Kumar, *Proc. of ASID '06, 8-12 Oct, New Delhi*, 2006, **6**, 388.

13 P. Peumans, S. Uchida and S. Forrest, *Nature*, 2003, **425**, 158–162.

14 V. Coropceanu, J. Cornil, D. da Filho, Y. Olivier, R. Silbey and J.-L. Brédas, *Chem. Rev.*, 2007, **107**, 926-952.

15 M. Premila, C. S. Sundar, P. Ch. Sahu, A. Bharathi, Y. Hariharan, D. V. S. Muthu and A. K. Sood, *Solid State Commun.*, 1997, **104**, 237-242.

16 J. Sakai, T. Taima, T. Yamanari and K. Saito, *Sol. Energ. Mat. Sol. C.*, 2009, **93**, 1149-1153.

17 H. Li, T. Earmme, S. Subramaniyan and S. A. Jenekhe, *Adv. Energy Mater.*, 2015, **5**, DOI: 10.1002/aenm.201402041.

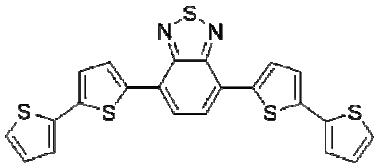

DT

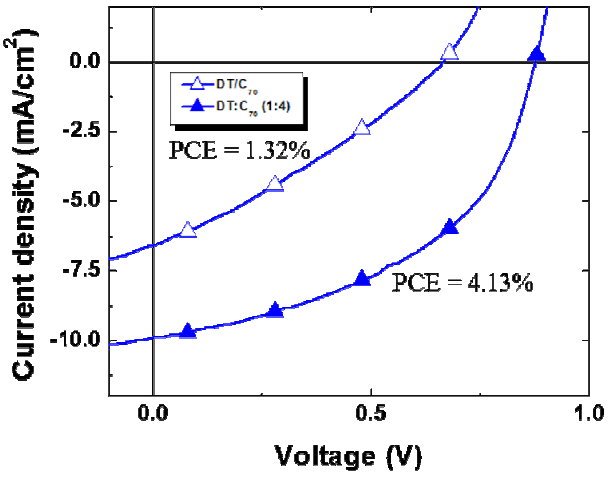

The bulk heterojunction device based on **DT**:C_{70} = 1:4 exhibited an efficient power conversion efficiency of 4.13%.